Journal of Earth Science, *Vol. 27*, *No. 5*, *p. 823–834*, *October 2016* *ISSN 1674-487X*
Printed in China
DOI: 10.1007/s12583-016-0705-5

Sedimentary Characterization of the Upper Paleozoic Coal-Bearing Tight Sand Strata, Daniudi Gas Field, Ordos Basin, China

Wei Du*[1], Zaixing Jiang[2], Qing Li[2], Ying Zhang[3]
1. *Petroleum Exploration and Production Research Institute of SINOPEC*, *Beijing* 100083, *China*
2. *College of Energy*, *China University of Geosciences*, *Beijing* 100083, *China*
3. *Research Institute of Petroleum Exploration and Development*, *PetroChina*, *Beijing* 100083, *China*

ABSTRACT: The coal-bearing strata of the Upper Paleozoic (from the Taiyuan Formation to the lower member of the Shanxi Formation) are the most important units that have high gas production in the Daniudi gas field, which is a typical tight-sandstone reservoir with high heterogeneity in the Ordos Basin, China. Based on an integrated investigation of well logs, cores, SEM and 3-D seismic data, we delineated the sedimentary facies of the coal-bearing strata and divided the succession into sequenced stratigraphic units of different depositional systems. A sedimentary hiatus was documented for the first time in the study area and forms the sequence boundary between the Lower Pennsylvanian Carboniferous Taiyuan Formation ($C t_1$) and the Upper Pennsylvanian Carboniferous Taiyuan Formation ($C t_2$). The coal-bearing strata in $C t_1$ are indicative of a barrier coastal deposition system. Tidal channels are identified by their fine-grained, cross-stratified character. The sands in the tidal channels are well sorted, and the quartz content is above 95%. The coalbed located beside the sandstone is thought to be a lagoon. Gas-bearing, coarse-grained sandstone in the coal-bearing strata spanning from the $C t_2$ to the lower members of the Shanxi Formation ($P_1 s$) is interpreted as a fluvial-dominated braided delta that is divided into four third-order sequences. The coal-bearing strata are composed of sandstone, mudstone and coalbed from base to top in each sequence. Braided-river deposits form the lowstand system tract (LST) within each sequence. A shelf and lake depositional environment containing dark gray mudstone forms the transgressive systems tract (TST). The highstand systems tract (HST) deposits form the swamp coalbed in each sequence.

KEY WORDS: sedimentary characterization, depositional system, Ordos Basin, highstand system tract.

1 INTRODUCTION AND GEOLOGICAL BACKGROUND

The Ordos Basin is located in the western part of the North China plate. It is composed of six structural units: the Yimeng uplift, western edge overthrust belt, Tianhuan depression, Yishan ramp, Jinxi flexural belt, and Weibei uplift (Cao, 2005; Chang et al., 2004). The Daniudi gas field, the focus of this article, is located in the northeastern Yishan ramp and have an area of approximately 2 003 km^2 (Fig. 1).

The Upper Paleozoic (from the Taiyuan Formation to the Shanxi Formation) was deposited under a very gentle paleo-topographic setting (high in the north and low-lying in the south) (Chen et al., 2004; Wang et al., 2002; Wang and Shen, 2000). The Carboniferous succession is composed of Benxi Formation and the overlying lower member of the Taiyuan Formation (Pennsylvanian). The Lower Permian succession is composed of the upper member of the Taiyuan Formation and the Shanxi Formation. The Taiyuan Formation and the lowest member of the Shanxi Formation provide the most important gas plays in Daniudi gas field. Gas production from a single well ranges of 0.5×10^4–10×10^4 m^3/d (Hao et al., 2006).

The thickness of the Taiyuan Formation ranges of 20–90 m, and the formation consists of member 1 ($C t_1$) and member 2 ($C t_2$; Fig. 2) of the Pennsylvanian Taiyuan Formation. The $C t_1$ primarily consists of medium to coarse-grained quartz sandstone, thick coal beds, and mudstones, whereas $C t_2$ mainly consists of conglomerate; gravelly; and coarse-, medium-, and fine-grained sandstones as well as limestones, coal beds, and mudstones.

The Shanxi Formation varies in thickness of 100–120 m and consists of three sub-members, $P_1 s_1^1$, $P_1 s_1^2$ and $P_1 s_1^3$ (Fig. 2). The first sub-member, $P_1 s_1^1$, consists of medium- to coarse-grained sandstones, thick coalbeds and mudstone, whereas $P_1 s_1^2$ and $P_1 s_1^3$ mainly consist of conglomerate, gravelly, and coarse-grained sandstones with thin coalbeds and mudstones. The siliciclastic sediments were primarily derived

*Corresponding author: duweiamy@163.com

Manuscript received October 28, 2014.
Manuscript accepted November 3, 2015.

Du, W., Jiang, Z. X., Li, Q., et al., 2016. Sedimentary Characterization of the Upper Paleozoic Coal-Bearing Tight Sand Strata, Daniudi Gas Field, Ordos Basin, China. *Journal of Earth Science*, 27(5): 823–834. doi:10.1007/s12583-016-0705-5. http://en.earth-science.net

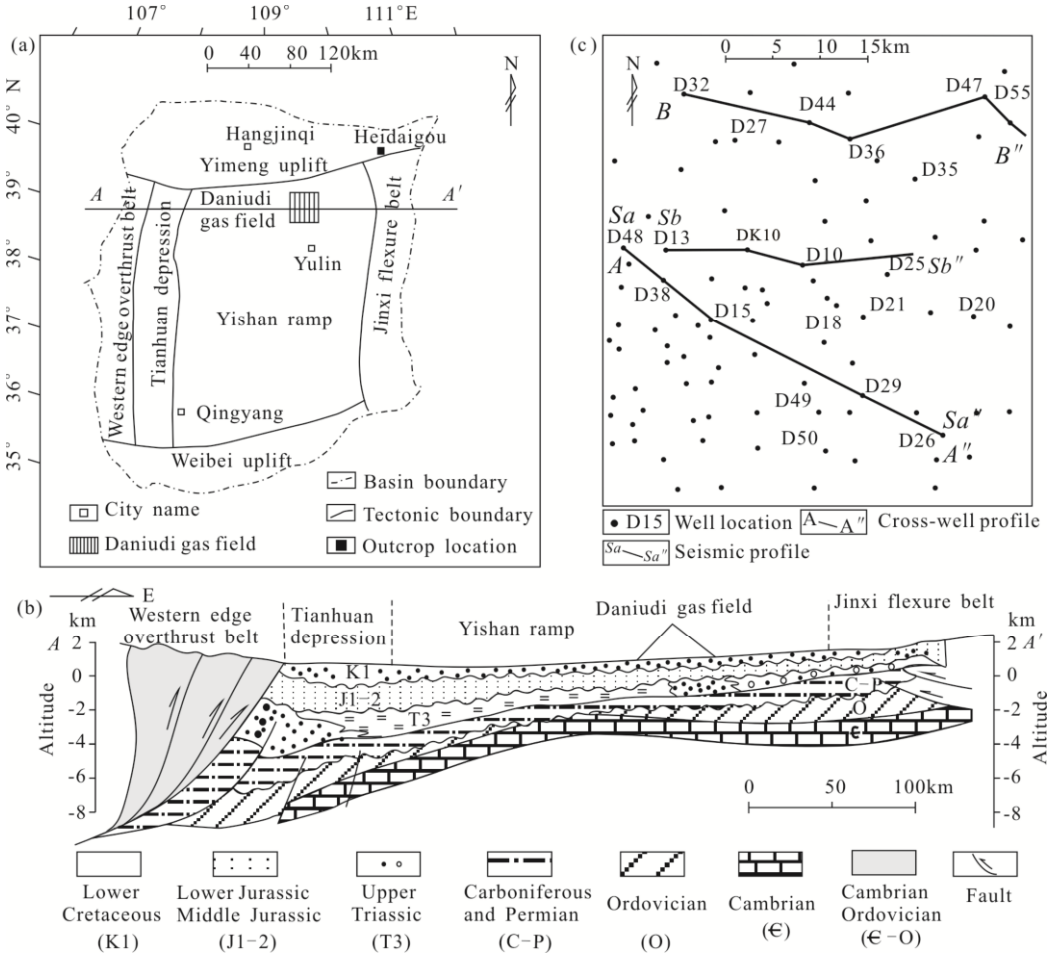

Figure 1. (a) Structural divisions of the Ordos Basin (modified from Yang et al., 2005); (b) geologic structure cross section of the Ordos Basin (modified from Yang et al., 2005); (c) well locations and cross-well profiles shown in Fig. 6a and seismic profiles shown in Fig. 6b of the Daniudi gas field.

from the Yimeng uplift in the northern part of the Ordos Basin during the Late Paleozoic era (Dou et al., 2009; Liu et al., 2003).

The Ct_1 contains a prominent barrier island-lagoon system facies association (Hao et al., 2007; Chen et al., 2004). Wang et al. (2007) suggested that the depositional environment had transitioned to barrier shoreline and braided delta-plain deposits by the late Ct_2. Others have proposed that Ct_2 is composed of deltaic deposits (Fu et al., 2003) or thin shallow-marine limestones with thick fluvial-deltaic deposits (Liu, 1998; Li et al., 1995). Based on the study of fusulinid bearing strata, Guo and Liu (1999) suggested that abrupt, high-frequency sea level changes were characteristic of the Late Paleozoic, and the Taiyuan Formation contains a record of such relative sea level changes.

Many researchers have proposed that the sedimentary system in the Shanxi Formation is a deltaic-fluvial. Zhang et al. (2011) suggested that the Lower Shanxi Formation was deposited under an epicontinental environment as indicated by the marine fossils.

2 DATABASE AND METHODOLOGY

This work was conducted using cores and 200 thin sections from 20 wells and well logs and gas production data from 120 wells. Three outcrops were also examined using nearly 2 000 km^2 of three-dimensional seismic data. Detailed core and thin section descriptions and precise measurements of well-exposed outcrops allow us to identify the sedimentary microfacies within the Taiyuan Formation. Well tie correlations and seismic interpretations allow onlap at the sequence boundary and both along-strike and downdip geometries in the overlying incised valley to be identified.

3 SEDIMENTARY FACIES

3.1 Sedimentary Characteristics of SQ1

The deposits in Ct_1 primarily consist of coal beds; mudstones; and fine-, medium-, and coarse-grained sandstones (Fig. 3a). The lower part of Ct_1 (Fig. 3a), which ranges of 2 575–2 581 m, consists of fine-grained sandstone deposits in a fining-upward succession. The grains are subangular, moderately to well sorted, and contain 92% content of quartz. This succession begins with parallel beddings, followed by flaser and lenticular beddings (Fig. 3b). These characteristics indicate a strong tidal influence, and this succession may represent tidal channel deposits.

The middle of Ct_1 (Fig. 3a), which ranges of 2 564–2 574 m, is separated from the lower part by an approximately 1-m-thick black lagoonal mudstone. This section is mainly composed of gravelly, coarse-grained sandstone and medium- to coarse-grained sandstones. The grains are subangular and well sorted with extremely high quartz content (almost 99%).

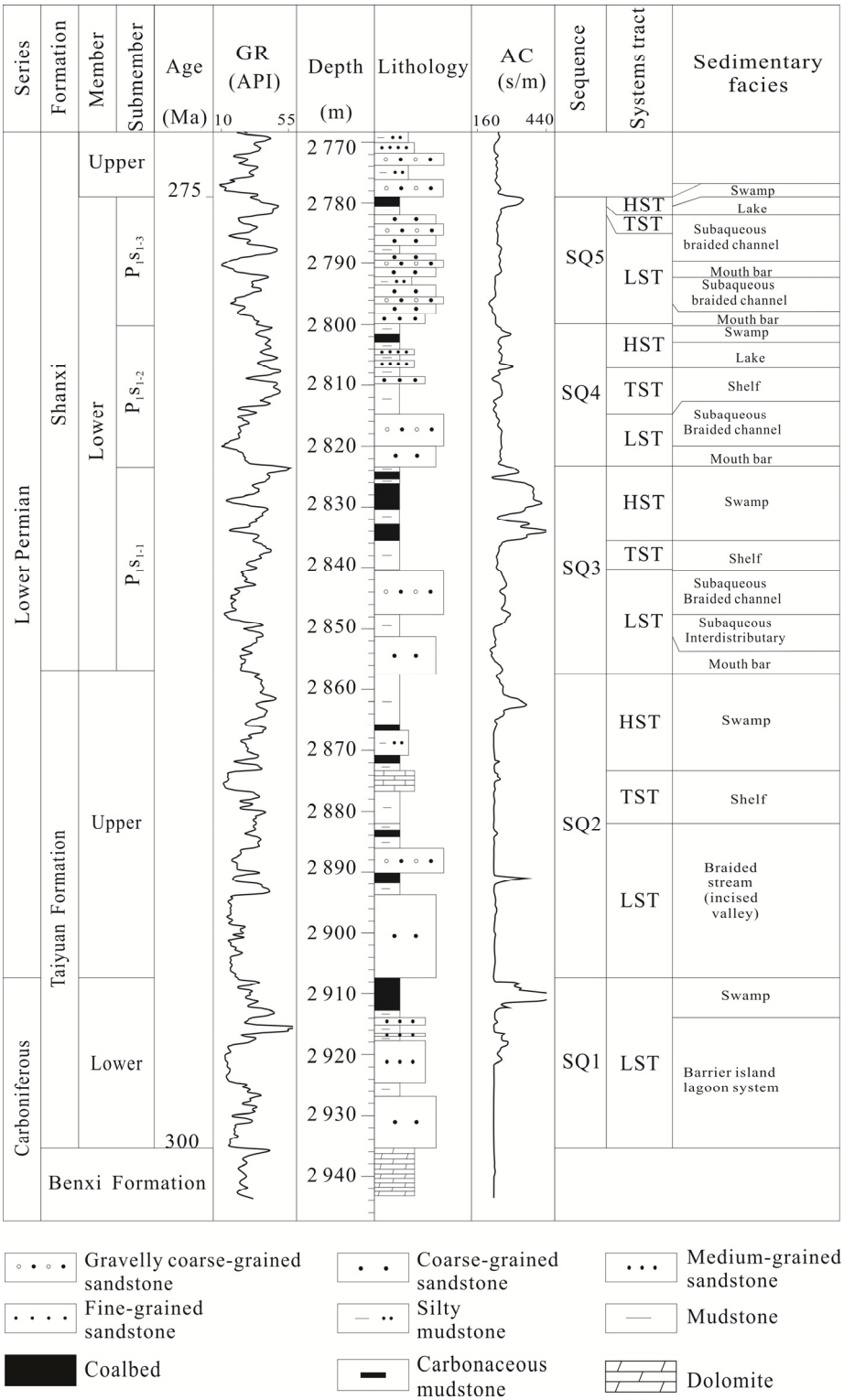

Figure 2. Lithology, sedimentary facies, and sequence stratigraphic divisions of the Taiyuan Formation and the lowest member of Shanxi Formation in the Daniudi gas field. LST. Lowstand system tract; TST. transgressive system tract; HST. highstand system tract.

The succession fines upward from the gravelly coarse-grained sandstone at its base to medium- to fine-grained sandstone. Parallel bedding, low-angle cross-bedding (Fig. 3c), and trough cross-bedding (Fig. 3d) are all present and may be tidal channel deposits.

The uppermost deposits in Ct_1, which range of 2 555–2 564 m, are composed of thick coal beds and thin black carbonaceous mudstones (Fig. 3e). The predominant sedimentary environment of the Taiyuan Formation is a barrier shoreline (Hao et al., 2007; Wang et al., 2007; Chen et al., 2004), and the primary sedimentary facies in Ct_1 are from barrier islands, tidal channels, and lagoons. Tidal channels are identified by their fine-grained, cross-stratified character (e.g., Ni et al., 2015). Some crossstratification suggests bidirectional paleocurrents (Figs. 4a, 5a). The sands are well

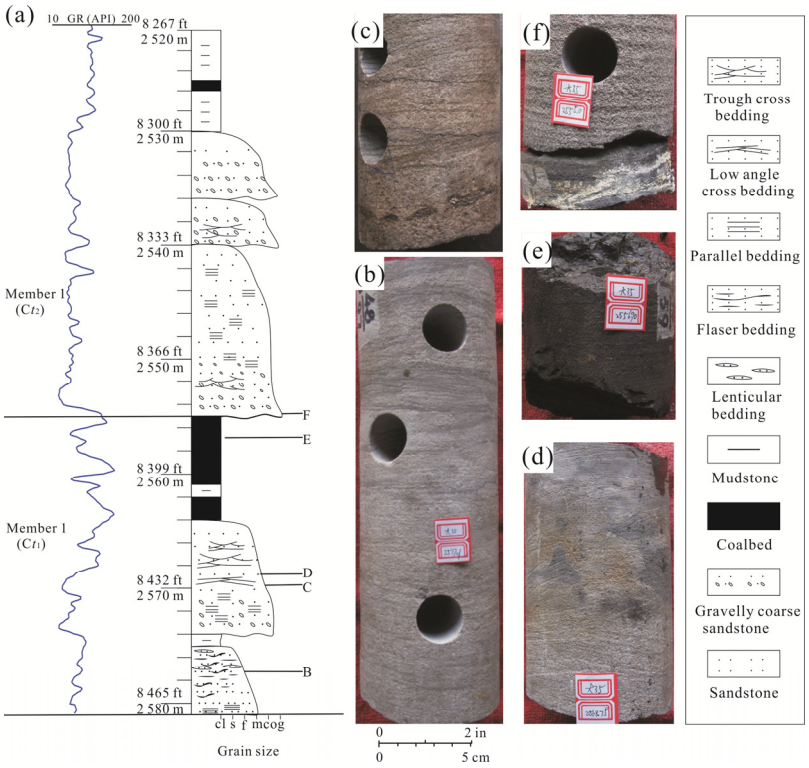

Figure 3. Detailed description of the lithology and sedimentary structure within the Taiyuan Formation based on cores (Well D35, from 2 520–2 581 m). (a) Lithologic log; (b) fining-upward fine-grained sandstone with paralleled bedding, flaser bedding, and lenticular bedding; (c) low-angle cross-bedding; (d) trough cross-bedding; (e) coal bed; (f) scour surface and coarse-grained sandstone eroding the underlying coal bed. The coarse-grained sandstone overlies a scour surface and has eroded the underlying coalbed. The core locations are shown to the left of each photo. cl. clay; s. siltstone; f. fine-grained sandstone; m. medium-grained sandstone; co. coarse-grained sandstone; g. gravelly sandstone.

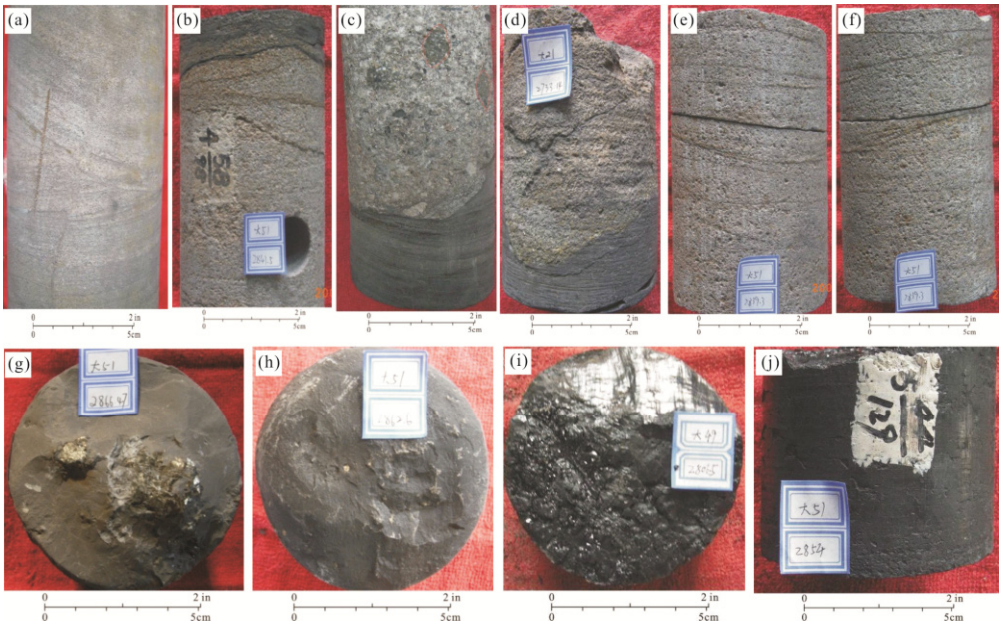

Figure 4. Core photographs of the sedimentary structures of Ct_1 and Ct_2. (a) Possible Herringbone cross-bedding, which suggests a tidal current (Well D23, 2 794 m). (b) The medium-grained sandstone coarsens upwards to a coarse-grained sandstone. This upward-coarsening succession is interpreted as a barrier island deposit. Parallel bedding occurs of the lower part and trough cross-bedding occurs in the upper part (Well D51, 2 844 m). (c) An upward-fining succession in a conglomerate. The coarsest clasts are approximately 3 cm in diameter and some appear to be imbricated. The scour surface is in the middle of the core and overlies the horizontally bedded mudstone (Well D55, 2 468 m). (d) Gravelly coarse-grained sandstones overlie the gray mudstone at one erosional contact (Well D21, 2 733 m). (e) Trough cross-bedding (center of the core) and parallel bedding (upper part of the core; Well D51, 2 839.3 m). (f) Wedge-shaped cross-bedding (Well D51, 2 839.3 m). (g) and (h) Black mudstone containing pyrite (Well D51, 2 866.47 m; Well D51, 2 862.8 m), (i) and (j) Coal beds formed in a lagoon-swamp environment (Well D49, 2 808 m; Well D51, 2 854 m).

sorted, and the quartz content of the tidal channel sands is over 95% (Jiang et al., 2012).

The barrier island facies are primarily composed of moderately to well sorted eolian trough cross-bedded medium-grained sandstones with a coarsening-upward vertical motif (Fig. 4b). There were well-sorted sandstones from the barrier islands in the western Gulf of Mexico. A significant characteristic of the barrier island deposits within Ct_1 is their high compositional maturity and average quartz content of over 95% (Jiang et al., 2012).

Lagoon and swamp deposits form the major fine-grained components in Ct_1. These deposits are mainly composed of coal beds and carbonaceous mudstones (Figs. 2, 3). Dark lagoonal mudstones contain pyrite (Figs. 4g, 4h). Coal beds are common in the upper part of Ct_1 (Figs. 3, 4i, 4j), with thicknesses ranging of 6–16 m.

3.2 Sedimentary Characteristics of SQ2

The Ct_2 deposits can also be divided into three parts. A lower interval of coarse-grained sandstones overlain by mudstone and limestone intervals are followed by an upper mudstone, coal bed, and fine-grained sandstone section (Fig. 2). The lower part of the Ct_2, of 2 530–2 555 m, is composed of multiple fining-upward successions (Fig. 3). Each succession begins with a scour surface at its base, which indicates an erosion of the underlying strata. During the first fining upward succession of 2 540–2 555 m, the 10 m of gravelly coarse-grained sandstones with trough cross-bedding is overlain by 5 m of medium- to coarse-grained sandstones with parallel bedding. The gravelly, coarse-grained sandstone is subangular, moderately well sorted and 88% quartz. Gravel clasts with 4 to 6 mm in diameter account for 20 to 50% of the gravelly coarse sandstone. Two other fining-upward cycles of 2 530–2 540 m have scour surfaces at their base. Trough cross-beddings are the primary sedimentary structures (Fig. 3f). These coarse-grained sandstones, which compose the lower part of Ct_2, are overlain by thick layers of mudstone (Fig. 3a) or limestone (Fig. 2). These layers are in turn overlain by the upper part of Ct_2, which is primarily composed of thin coalbed, mudstone (Fig. 3), siltstone, and fine-grained sandstone (Fig. 2).

These coarse-grained sediments are interpreted as braided stream deposits lying directly on the underlying coal beds or carbonaceous mudstones in Ct_1 (Figs. 2, 3, 4c, 4d). Some gravels contain high angle cross strata and erosional surfaces, which indicates the sediments were deposited from strong, confined tractive currents capable of moving subaqueous gravel dunes (Fig. 4c). The fining-upward character of these sharp-based fluvial deposits can also be recognized in the outcrops.

In addition, trough cross-bedding, plane-parallel lamination, wedge cross-bedding, and planar cross bedding are all observed in both cores (Figs. 4e, 4f) and the outcrops (Jiang et al., 2012). The gamma-ray log of the braided stream deposits is a typical cylindrical shape (2 794–2 808 m; D49, Fig. 2).

Many erosional surfaces were observed within these braided stream deposits. The braided stream sand bodies in Ct_2 directly erode the coal bed and car bonaceous mudstones in the underlying Ct_1. The high relief of the scour surfaces was caused by this erosion. Some scour surfaces within the braided stream gravels also erode the fine- and medium-grained sandstones in Ct_1 (Jiang et al., 2012).

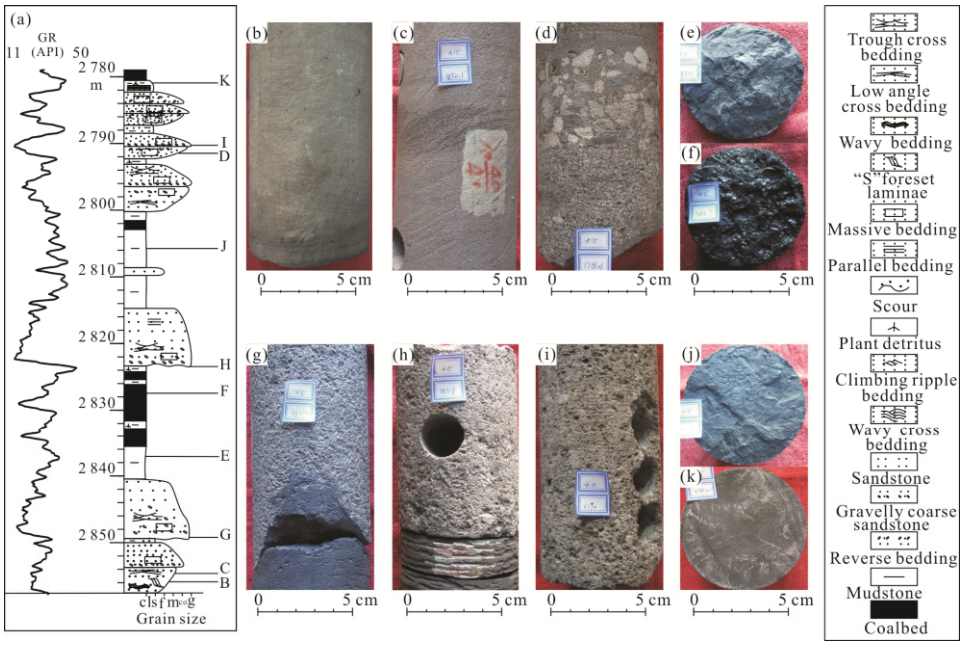

Figure 5. Detailed descriptions of the lithology and sedimentary structures within the lower member of the Shanxi Formation based on the obtained cores (Well D15, from 2 780 m to 2 858 m). (a) Lithologic log; (b) low-angle cross-bedding; (c) "S" foreset laminae; (d) fining-upward succession; (e) mudstone from $P_1s_1^1$; (f) coalbed from $P_1s_1^1$; (g) scouring surface and coarse-grained sandstone eroding the underlying mudstone in $P_1s_1^1$; (h) scouring surface in $P_1s_1^2$; (i) massive bedding; (j) mudstone in $P_1s_1^2$; (k) mudstone in $P_1s_1^3$. Locations are shown to the left of each photo. cl. clay; s. siltstone; fine. fine-grained sandstone; m. medium-grained sandstone; co. coarse-grained sandstone; g. gravelly sandstone.

The matrix of the braided-stream clastic sediments is high in the thin sections (as much as 20%–30%). The grains are angular and poorly sorted, which indicates a short transport distance. In contrast, the clastic particles from the barrier shoreline setting are affected by tides, waves, and winds and thus better sorted and more rounded (Jiang et al., 2012).

The widespread shelf mudstones and limestones overlying the braided stream deposits indicate a sea level rise. The limestones and mudstones are overlain in turn by thin coalbed units and the associated carbonaceous mudstones and silty sandstones, which all probably represent swamp deposits.

3.3 Sedimentary Characteristics of SQ3

Deposits in $P_1s_1^1$ are primarily sandstone, mudstone and coalbeds (Fig. 5a). The sandstone, which ranges of 2 840 to 2 857.5 m, can be divided into three parts. The lower part, ranging from 2 853.7 to 2 857.5 m, contains coarse- and medium-grained sandstones with a coarsening-upward succession. The succession begins with a low-angle cross-bedding followed by "S" foreset laminae (Figs. 5b and 5c). This part of the sandstone is considered to be a mouth-bar deposit from the braided delta front.

The middle of the coarse-grained sandstone forms a fining-upward succession with an initial massive beddings followed by a trough cross-bedding. The grains are subangular and moderately sorted. The uppermost coarse-grained sandstone is separated from the middle section by approximately 0.5 m of dark gray silty mudstone (Fig. 5g), and the main succession has a massive bedding (Fig. 5h). The GR log for the upper part of the coarse-grained sandstone is the typical cylindrical shape (2 840.5–2 849.5 m, D15, Fig. 5). The characteristics of these two fining-upward sandstones indicate a subaqueous braided-channel facies.

The mudstone overlying the sandstone ranges from 2 835.5 to 2 840.5 m and contains a small amount of carbonaceous clasts and plant stems (Fig. 5e). Some crinoids and foraminifera debris were found in the dark-gray mudstone (Zhang et al., 2011). These characteristics indicate that the mudstone was deposited from a marine environment. The sea level rose, and the mudstones were created from a shelf deposit.

The uppermost $P_1s_1^1$ deposits, which range from 2 823.5 to 2 835.5 m, comprise three thick coalbeds and two thin black carbonaceous mudstones (Fig. 5f). These deposits were formed from a stable swamp environment.

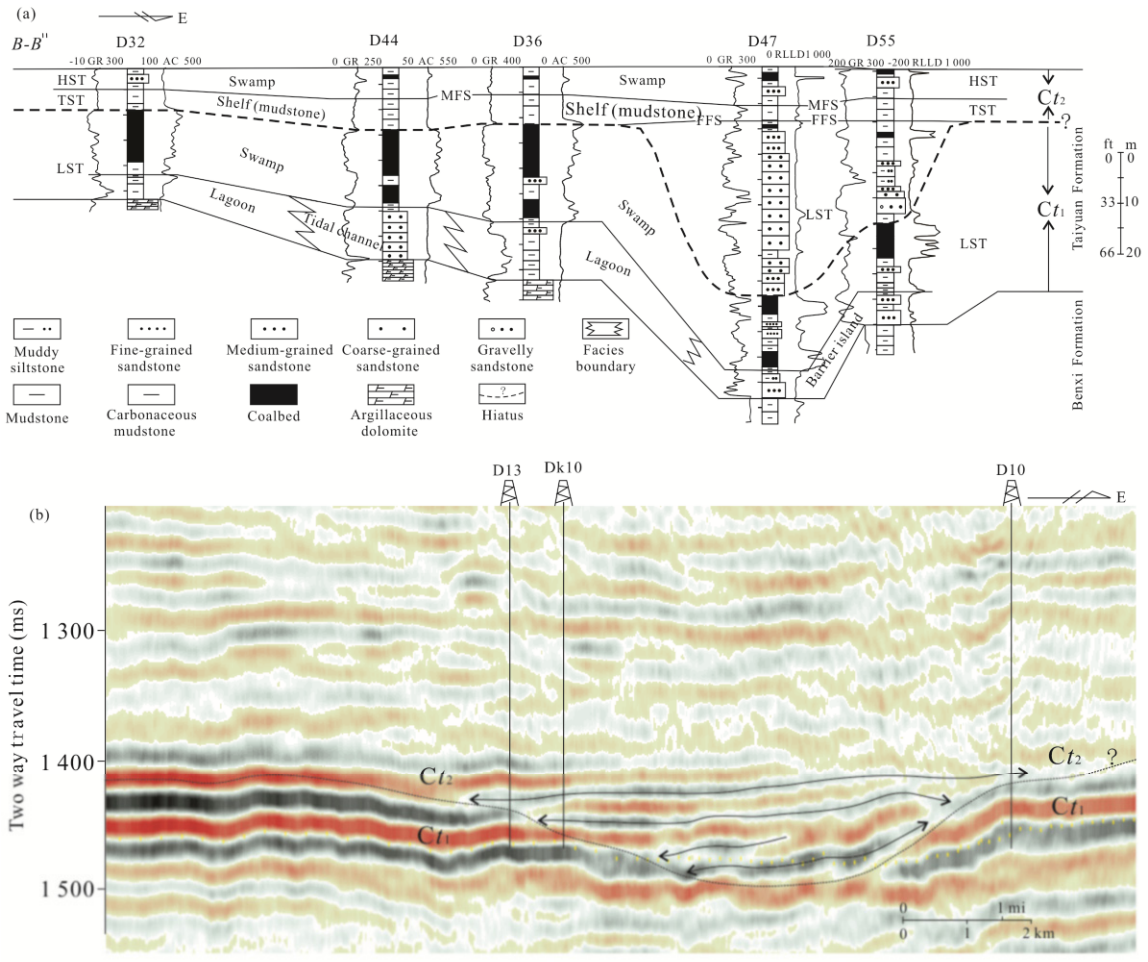

Figure 6. Cross-well profiles showing the facies stacking patterns, lateral trends, coal bed thickness variations, and incised-valley geometry. (a) Cross-well profiles are perpendicular to the incised valley when oriented east to west; (b) seismic image of the incised valley in the Daniudi gas field with a concave base and onlapping channell. See Fig. 1c for the location of these wells. FFS. first flooding surface; MFS. maximum flooding surface; LST. lowstand systems tract; TST. transgressive systems tract; HST. highstand systems tract; GR. gamma ray; RLLD. resistivity; AC. acoustic.

3.4 Sedimentary Characteristics of SQ4

The deposits in $P_1s_1^2$ deposits range from 2 800 to 2 823.5 m and can be divided into three parts (Fig. 5a). The lower part consists of sandstone with a fining-upward succession and ranges from 2 823.5 to 2 815 m. This sandstone erodes the carbonaceous $P_1s_1^1$ mudstones (Fig. 5h). These sandstones are primarily massive, gravelly, coarse, and poorly sorted but with high roundness. The particle size of the gravels ranges from 2 to 3 mm. The gravelly sandstone has a little matrix and is particle-supported, which indicates a subaqueous braided-channel deposition.

The middle part of the $P_1s_1^2$ consists of mudstone and ranges from 2 803 to 2 815 m. The lithology is mostly grayish-green, gray and chromocratic mudstones with little silty mudstone (Fig. 5j). Zhang et al. (2011) determined from the electron-probe analysis that the Mg/O content of the siderite in the mudstone sample is approximately 0.5%–7.8%, which indicates a shelf depositional environment.

The uppermost part of $P_1s_1^2$, which ranges from 2 800 to 2 803 m, contains coalbeds and thin black carbonaceous mudstones (Fig. 5a). In contrast to $P_1s_1^1$, the thickness of the coalbed in the upper part of $P_1s_1^2$ is 3 m and decreases sharply. These observations indicate a swamp depositional environment.

3.5 Sedimentary Characteristics of SQ5

Deposits in $P_1s_1^3$ range from 2 779.5 to 2 800.5 m and are mainly conglomerate, sandstones, mudstone and coalbed (Fig. 5a). These deposits can be divided into four parts. The first three parts form a coarsening-upward succession followed by a fining-upward succession. The fourth part of the sandstone forms a fining-upward succession.

The first part of the coarsening-upward succession, which ranges from 2 796.5 to 2 800.5 m, is a coarse-grained sandstone with mudstone rips (Fig. 5a). The grains are subangular and moderately sorted. The upper sandstone, which ranges from 2 793.5 to 2 796.5 m, contains gravelly coarse and conglomerate sandstones with a fining-upward succession. The succession of the second part of the sandstone is the same as that of the first, a coarsening-upward succession ranging from 2 788.5 to 2 792.5 m (Fig. 5d) followed by a fining-upward succession ranging from 2 788.5 to 2 790.5 m with 5 cm-thick gravelly strips supported by particles and overlain with 2 m of the conglomerate with massive bedding (Fig. 5i). The third part was also a fining-upward succession and ranged from 2 784.5 to 2 787.5 m. The fourth part of the deposit is a fining-upward succession ranging from 2 782.5 to 2 783.5 m. The channel-floor conglomerate has little matrix and is particle-supported. The middle section of $P_1s_1^3$, 2 780.5 to 2 782.5 m, contains mudstone with carbonaceous clasts (Fig. 5k). Some crinoids and foraminifera debris were found in the mudstone; however, less than for $P_1s_1^1$. These findings indicate that the mudstone was deposited under a marine environment. The uppermost section of $P_1s_1^3$, from 2 779.5 to 2 800.5 m, is a 1 m thick coalbed, which indicates a swamp depositional environment.

All of the deposits with coarsening-upward successions are indicative of mouth-bar deposits, while fining-upward successions indicate a subaqueous, braided-channel deposition. In addition, carbonaceous mudstone and coalbeds formed from swamps.

Based on our observations of the cores and examination of the well-log response data, we suggest that the lower members of the Shanxi Formation were deposited in the following sedimentary facies or subfacies: subaqueous braided channel, subaqueous interdistributary, mouth bar, swamps and shelf.

The braided delta contains megaclast and is controlled by a braided-river system rich in sand and gravel (Jiang, 2003). The mouth bar was mostly deposited at the end of the subaqueous braid channel. The subaqueous braided channels represent the most active part of the distributive channel network and are intimately associated with the mouth bars (Cornel and Janokp, 2006). The mouth bar in the study area contains fine-, medium- and coarse-grained sandstones. Sandstones in such mouth-bar deposits have a coarsening-upward succession with cross-beddings and "S" foreset laminae (Figs. 5b, 5c and 5d). The sandstones in the subaqueous braided channels were deposited in a fining-upward succession with massive bedding (Figs. 5g, 5h and 5i).

3.6 Stacking Patterns and Lateral Trends in SQ1 and SQ2

There are four stacking patterns for Ct_2 facies that overlie those of Ct_1: a barrier island overlain by a braided stream, a swamp overlain by braided stream, a swamp overlain by shelf limestone, and swamp overlain by shelf mudstone.

The first two stacking patterns, a basinward shift in the facies or a barrier island and swamp both overlain by a braided stream, indicate an abrupt progradation and fall in sea level. The carbonaceous mudstones and coal beds in erosive contact with the overlying conglomerate and coarse-grained sandstones are common in the study area (Figs. 6a, 6b). Fine-grained sandstones from the barrier island facies and eroded by gravels were seen in the cores.

In contrast, the second set of stacking patterns were represented by the shelf mudstone and overlying limestone swamp deposits, which indicate a landward facies shift caused by a relative rise in the sea level. These relationships are shown in the cross-well profile (Fig. 6a).

The vertical facies stacking pattern and lateral facies trend shown in Fig. 8 illustrate that the Ct_2 braided stream sediments eroded a relatively limited area of the underlying coal beds and carbonaceous mudstones in Ct_1 and were overlain in turn by the shelf limestone or mudstone. In contrast, the swamp in Ct_1 was directly overlain by a wide area of the shelf limestone or mudstone in Ct_2 where the braided stream facies is absent. It is therefore possible that the braided stream facies in Ct_2 had eroded over a part of the study area which created a hiatus between Ct_1 and Ct_2. We will investigate this possibility further in the following section based on outcrop observations, outcrop correlations, seismic interpretations, and changes in the coalbed thickness.

3.7 Stacking Patterns and Lateral Trends in SQ3, SQ4 and SQ5

As stated above, three sequences exist in the lower member of the Shanxi Formation. The vertical lithology of each sequence involved overlapped sandstone, mudstone and coalbed (Fig. 2). The sandstone primarily occurs in the sub-

aqueous braided channel and mouth bar of the braided delta front in the lower part of each sequence or sub-member. Dark gray mudstone shelf deposits form the middle part of each sub-member. The coalbed and carbonaceous mudstones imply a swamp depositional environment for the uppermost layer of each sub-member.

The lateral facies trends shown in Fig. 6 indicate that the subaqueous braided channels in the lower part of each sub-member extend to the northeast-southwest with the sway of the estuary in the braided delta front, which can be recognized in the seismic profile (Fig. 7b). The sandstone in the mouth bar was deposited at the end of the subaqueous braided channels. The braided delta-front depositional system in $P_1s_1^1$ creates deposits further from the shoreline than that for $P_1s_1^2$ and $P_1s_1^3$. As a result, the mouth bars were reworked more by the waves for $P_1s_1^1$ than in $P_1s_1^2$ and $P_1s_1^3$.

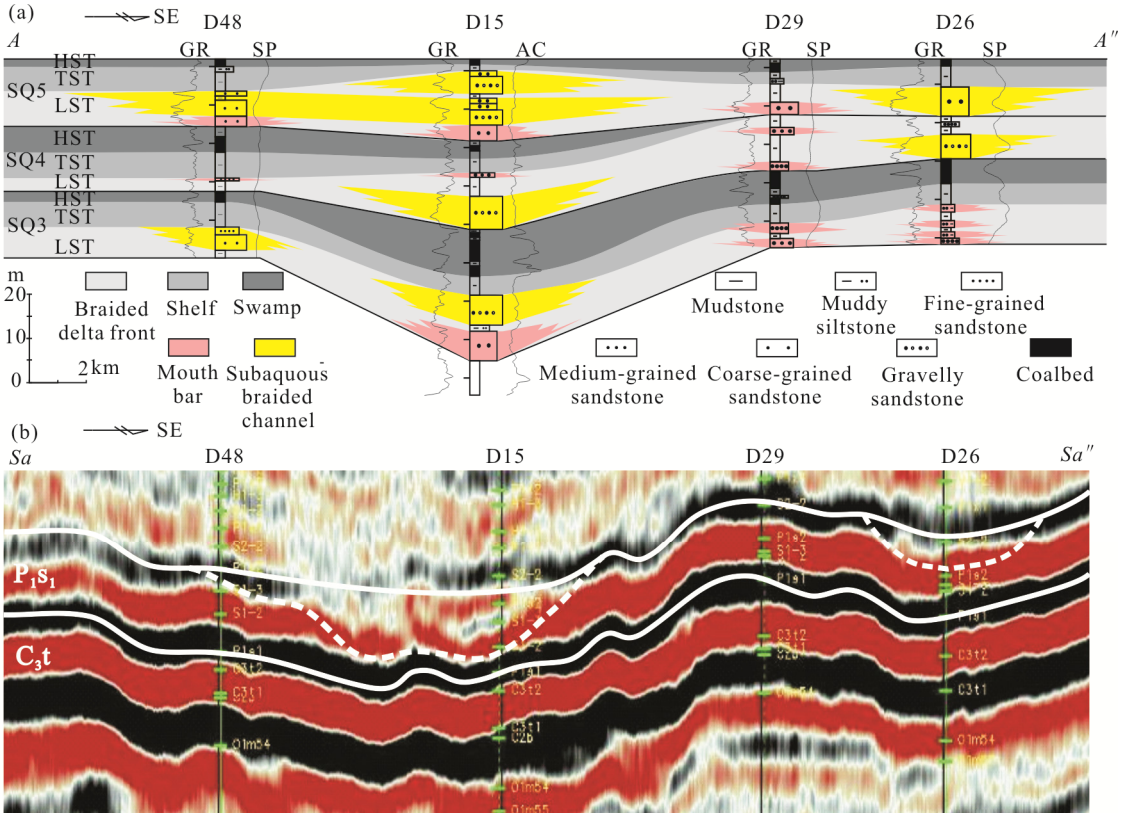

Figure 7. Sedimentary facies stacking patterns and lateral trends (NW-SE). (a) The cross-well profile was oriented northeast-southwest perpendicular to the subaqueous braided channel; (b) seismic-profiles responses. See Fig. 1c for location.

As shown in Fig. 7a, the subaqueous braided channel in SQ3 is only 2–3 km wide. In SQ5, this width reaches 6–8 km. The stacking of the subaqueous braided channels in the three sub-members is clearly reflected in the seismic profile (Fig. 7a). The extension of the subaqueous braided channels into the three sub-members forms an obvious progradational shape.

The progradational shape of the three sub-members, SQ3 to SQ5, is apparent in other ways. From the core observations, we found that the granularity and size of the sandstone succession varied regularly from the bottom to the top. The SQ3 sandstone was coarse-grained and contained little gravel with successions containing cross- and massive beddings. The sediments in SQ4 are gravelly and have a massive succession. The grain size of this gravel is 2–4 mm (Fig. 5h). The sediments in SQ5 are conglomerate and gravelly coarse sandstones with massive beddings (Fig. 5i). The quartz content of the thin sections decreases from SQ3 to SQ5, while the lithic content increases. In addition, the sandstone percentage increases as the mudstone decreases from SQ3 to SQ5.

The braided delta in $P_1s_1^1$ is the smallest of the three sequences or sub-members. The braided channels extend a short distance below sea level. Terrigenous sediments quickly deposit and form a mouth bar and interdistributary in the Daniudi gas field. The braided delta grows increasingly large as it extends into $P_1s_1^2$ and $P_1s_1^3$ (Fig. 5).

Based on the changes to the lithology, succession, clastic composition and vertical facies stacking patterns shown in Fig. 7, we propose that the braided delta is progradational in the three northeastern Ordos Basin sub-members.

4 RESULTS

4.1 Sedimentary Facies of LST in SQ1

A barrier shoreline depositional system that includes barrier islands, a tidal channel, and a lagoon developed in the lower part of Ct_1 (Fig. 8). These barrier islands extended in the northeast-southwest directions and were approximately 5–7 km wide. The tidal flow entered the lagoon through southeast-northwest oriented tidal channels. The lagoon promarily occupied the northwestern part of the studied area. This depositional system is interpreted as having developed during falling

sea levels and represents an early LST.

The coal accumulation is controlled by the tectonic setting, depositional environment, paleoclimate, and plant material availability (Han and Yang, 1980). The areas where the subsidence rates are either too low or too high are unfavorable for accumulating coal (Shao et al., 2003). Bohacs and Suter (1997) suggested that significant volumes of terrigenous organic matter can be preserved and only form coal when the overall increase in accommodation is approximately equal to the production rate of peat. This phenomenon most likely occurs within the LST and HST, where the sea level changes at a moderate rate.

Thick coal beds overlying the barrier shoreline deposits developed widely at the top of Ct_1 as the lagoon became swampy (Figs. 2, 3, and 8). The overall accommodation increase must, therefore, approximately equal the peat production rate at that time. This aggradational interval represents the late LST.

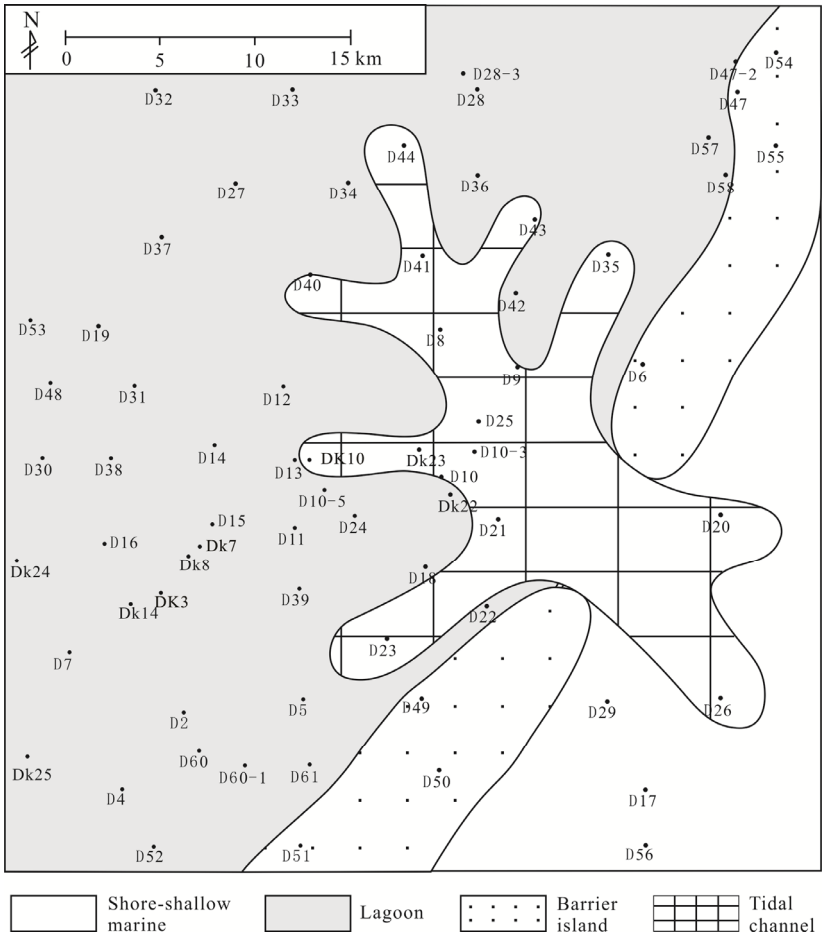

Figure 8. Sedimentary facies for the early lowstand system tract in SQ1. The barrier islands extended in a northeast-southwest direction and were approximately 5–7 km wide. The lagoon was mostly located in the northwestern part of the study area.

4.2 Sedimentary Facies of LST in SQ2

The sedimentary hiatus between Ct_1 and Ct_2 was accompanied by an incised valley at the base of Ct_2. The thick incised-valley, which was mostly filled with conglomerates and coarse- to fine-grained sandstones, is strong evidence of an LST. The incised valley is oriented in a northeast-southwest direction (Fig. 9). The strata outside the incised valley (beneath the hiatus) consisted of exposed coal beds from Ct_1. Erosion from the braided stream system resulted in the coal beds below the valley being thinner than those across the rest of the area.

4.3 Sedimentary Facies of LST in SQ3

Based on the sedimentary facies, the LSTs that were similar to each other in SQ3, SQ4 and SQ5 formed a progradational braided delta. The depositional environment of the LSTs from SQ3 in the lower member of the Shanxi Formation formed a braided delta front in the Daniudi gas field (Fig. 10). As shown in Fig. 10, the sedimentary facies form subaqueous braided channels with mouth bars and interdistributary environments.

5 DISCUSSION

The area from the Taiyuan Formation to the lower member of the Shanxi Formation was divided into five sequences, SQ1, SQ2, SQ3, SQ4 and SQ5. The LST deposits were sandstone from each sequence. The TST and HST deposits in SQ1 were eroded by the LSTs from SQ2. The TST deposits in SQ2, SQ3, SQ4 and SQ5 were mudstone deposited in the ocean or shallow lake in response to the rising of the relative sea level. The coalbed was also eroded by the LSTs from the upper sequence and formed the HSTs of each sequence.

The sandstone in the LSTs, mudstone in the TSTs and coalbed in the HSTs formed a trap in the gas fields of the Ordos Basin. According to statistical analysis, the distribution of wells with high gas production was quite different for the five sequences. The changes in the depositional environment of each sequence were controlled by the relative sea level and sedimentary source. The distribution of the coalbed was similar in each sequence.

The progradetion of the braided delta extended the coalbed to the center of the Ordos Basin. The gas products from the various wells in the gas field vary greatly. According to a statistical analysis, wells with gas production between 2×10^4–10×10^4 m^3/d are generally located in the mouth-bar sandstones in the south part of the gas field. Wells with gas production between 0.5×10^4–2×10^4 m^3/d are mainly located in the subaqueous braided channel sandstone in the north part of the gas field (Fig. 10).

According to this research and statistical analysis, the gas resources of the Daniudi gas field are from the clastic sediments coalbeds of the Upper Paleozoic (from the Taiyuan Formation to the lower member of the Shanxi Formation). Wells with greater gas production in the Taiyuan Formation were mainly distributed across the tidal bar and incised valley, which had a banded distribution in the northeast-southwest direction. Also, those in the lower members of the Shanxi Formation were generally distributed in the mouth bar, which was mostly in the southwestern part of the gas field.

The distribution of wells with high gas production rates were controlled by the thickness and extension of the coalbed. A barrier shoreline depositional system that includes barrier islands, a tidal channel, and a lagoon developed in the LST of SQ1. In contrast to SQ1, deposits in the LSTs for SQ2, SQ3, SQ4 and SQ5 were coarse sandstones deposited in the braided delta front due to the relatively low sea level.

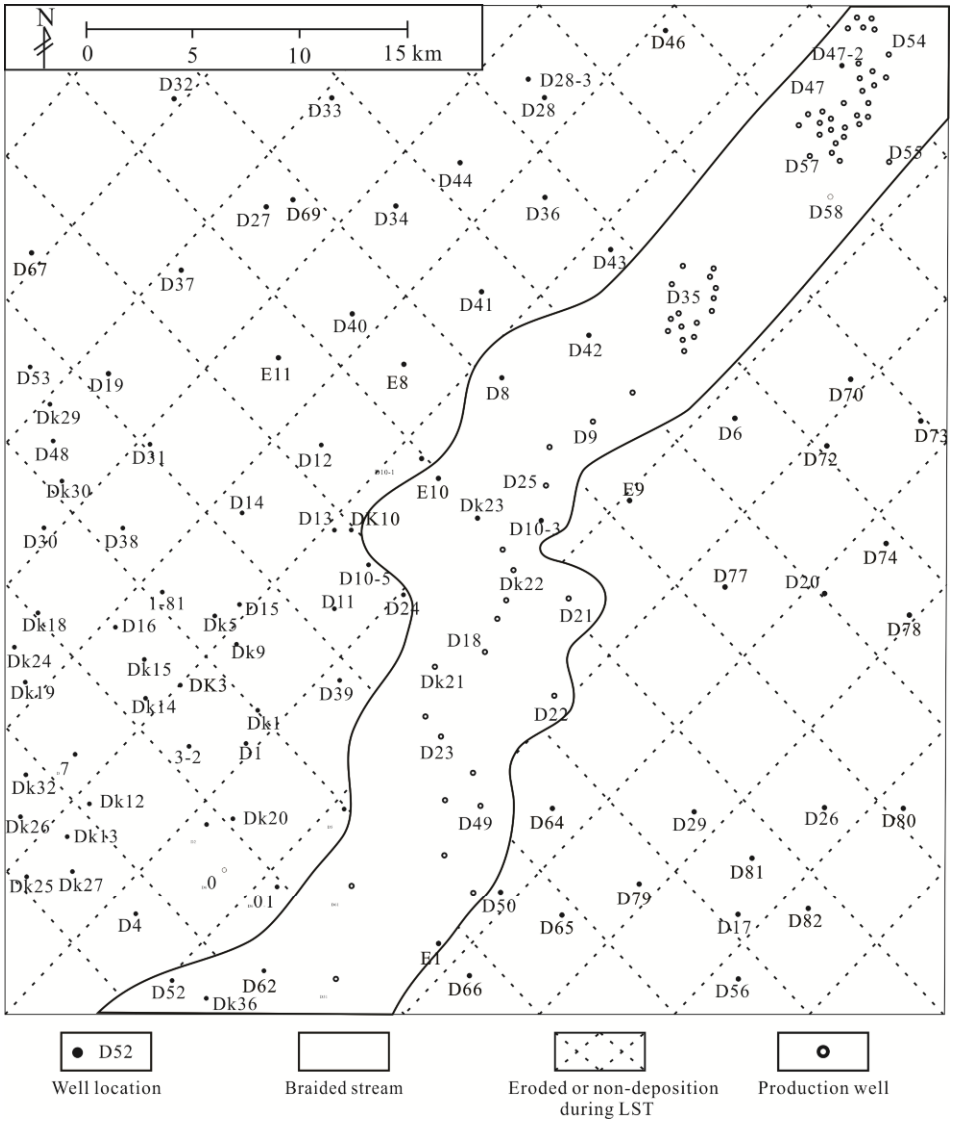

Figure 9. Sedimentary facies and gas productivition distribution in the lowstand systems tract (LST) of SQ2. The braided stream is oriented northeast to southwest. This figure also shows that the gas production wells are confined to the incised valley.

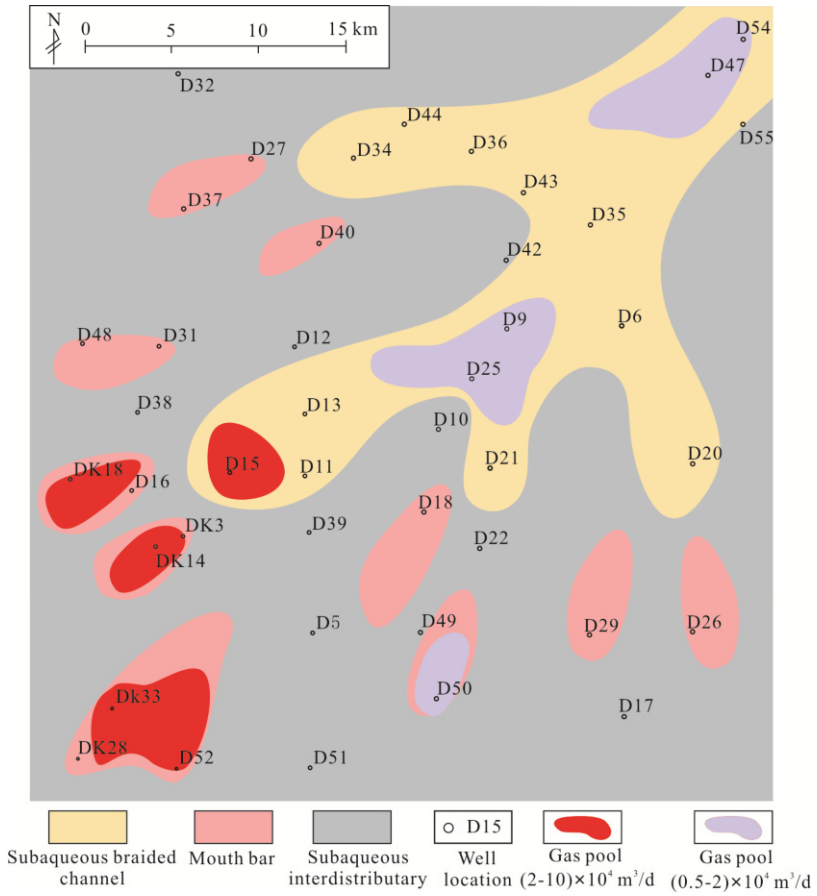

Figure 10. Sedimentary facies and distribution of gas productivity in the lowstand systems tract (LST) of SQ3.

6 CONCLUSIONS

Based on this sequence stratigraphy research, an erosional hiatus within the Taiyuan Formation was documented for the first time and represents a sequence boundary between the lower (Ct_1) and upper (Ct_2) members of the formation. There were three transgressive events above the Taiyuan Formation in the lower member of the Shanxi Formation in the Ordos Basin. The lower member of the Shanxi Formation was divided into three third-order sequences, SQ3, SQ4 and SQ5, in the Daniudi gas field. In addition, the braided delta-front deposits formed the LSTs for each sequence in the Daniudi gas field with the shelves as the TSTs and swamps as the HSTs.

The LST in Ct_1 had a barrier shoreline sedimentary environment overlain by thick swamp coal beds. These coal beds were then partly eroded, which created the sedimentary hiatus at the sequence boundary. The sequence boundary was overlain in turn by the lowstand incised-valley fill from Ct_2, which was interpreted from the seismic data and outcrop correlations and consisted of braided stream deposits as identified by the cores, well logs, and thin section descriptions. The TST of the overlying Ct_2 was dominated by limestone and mudstone, while the overlying HST contained swamp mudstone, thin sandstone, and coal beds.

The lower member of the Shanxi Formation deposited a progradational braided delta in the northeastern Ordos Basin with the following sedimentary facies or subfacies: subaqueous braided channel, subaqueous interdistributary, mouth bar, swamp and shelf.

Coarse clasts in the incised valley are the primary reservoirs of the studied area, and the valley geometry controls the gas reservoirs distribution. The coarse clasts of the incised-valley fill continue to be probable targets for future gas explorations both inside the study area and elsewhere in the Ordos Basin.

In the Daniudi Gas Field, the sand bodies from the mouth bar of the braided delta front, which form the LSTs in each sequence, make excellent reservoirs.

ACKNOWLEDGMENTS

This study was supported by the State Key Laboratory of Shale Oil and Gas Enrichment Mechanisms and Effective Development and the Key Laboratory of Shale Oil/Gas Exploration and Production of SINOPEC. We also thank Shiyue Chen, Longwei Qiu and Guoting Wang for their assistance in the research. The final publication is available at Springer via http://dx.doi.org/10.1007/s12583-016-0705-5.

REFERENCES CITED

Bohacs, K. M., Suter, J., 1997. Sequence Stratigraphic Distribution of Coaly Rocks: Fundamental Controls and Paralic Examples. *AAPG Bulletin*, 81: 1612–1639

Cao, Z. H., 2005. The Basic Geological Characteristics of the Daniudi Gas Field in Ordos Basin. *Journal of Southwest Petroleum Institute*, 27(2): 17–22 (in Chinese with Eng-

lish Abstract)

Chang, X. H., Wang, Y. B., Han, D. Q., 2004. Reservoir Characteristics of Lower Xiashihezi Formation in Daniudi Gas Field. *Natural Gas Industry*, 24(11): 19–21 (in Chinese with English Abstract)

Chen, J. L., Wu, L., Cui, J. J., 2004. The Sedimentography Characteristics of Daniudi Gas Field. *Journal of Jiaozuo Institute of Technology* (*Natural Science*), 23(2): 89–94 (in Chinese with English Abstract)

Cornel, O., Janokp, B., 2006. Terminal Distributary Channels and Delta Front Architecture of River-Dominated Delta Systems. *Journal of Sedimentary Research*, 76: 212–233

Dou, W. T., Hou, M. C., Dong, G. Y., 2009. Provenance Analysis of the Upper Paleozoic Shanxi to Lower Shihezi Formations in North Ordos Basin. *Natural Gas Industry*, 29(3): 25–28 (in Chinese with English Abstract)

Fu, S. T., Tian, J. C., Chen, H. D., et al., 2003. The Delta Depositional System Distribution of Late Paleozoic Era in the Ordos Basin. *Journal of Chengdu University of Technology* (*Science & Technology Edition*), 30(3): 236–241 (in Chinese with English Abstract)

Guo, Y. H., Liu, H. J., 1999. Transgression of Late Paleozoic Era in Ordos Area. *Journal of China University of Mining & Technology*, 28(2): 126–129 (in Chinese with English Abstract)

Han, D. X., Yang, Q., 1980. Coalfield Geology of China. In: Han, D. X., Yang, Q., eds., Coalfield Geology of China. China Coal Industry Publishing House. Beijing. 415 (in Chinese with English Abstract)

Hao, S. M., Li, L., You, H. Z., 2007. Permo-Carboniferous Paralic Depositional Systems in the Daniudi Gas Field and Its Near-Source Box-Type Gas Accumulation-Forming Model. *Geology in China*, 34(4): 606–611 (in Chinese with English Abstract)

Hao, S. M., Hui, K. Y., Li, L., 2006. Reservoiring Features of Daniudi Low-Permeability Gas Field in Ordos Basin and its Exploration and Development Technologies. *Oil & Gas Geology*, 27(6): 762–768 (in Chinese with English Abstract)

Jiang, Z. X., 2003. Sedimentology. In: Jiang, Z. X., Chen, S. Y., Yang, J. P., eds., Sedimentology. Petroleum Industry Press, Beijing. 76–90 (in Chinese with English Abstract)

Jiang, Z. X., Xu, J., Wang, G. T., 2012. The Discovery and Significance of a Sedimentary Hiatus within the Carboniferous Taiyuan Formation, Northeastern Ordos Basin, China. *AAPG Bulletin*, 96(7): 1173–1195

Li, S., Yang, S., Jerzykiewicz, T., 1995. Upper Triassic–Jurassic Foreland Sequences of the Ordos Basin in China. In: Dorobek, S. L., Ross, G. M., eds., Stratigraphic Evolution of Foreland Basins. *SEPM Special Publication*, 52: 233–241

Liu, S., 1998. The Coupling Mechanism of Basin and Orogenin the Western Ordos Basin and Adjacent Regions of China. *Journal of Asian Earth Sciences*, 16: 369–383

Liu, Y. E., Huang, Y. M., Wei, X. F., et al., 2003. Analysis of Provenance of Late Paleozoic in the Northern Ordos Basin and Its Geological Significance. *Journal of Mineralogy and Petrology*, 23(3): 82–86 (in Chinese with English Abstract)

Ni, L. T., Zhong, J. H., Shao, Z. F., et al., 2015. Characteristics, Genesis, and Sedimentary Environment of Duplex-Like Structures in the Jurassic Sediments of Western Qaidam Basin, China. *Journal of Earth Science*, 26(5): 677–689. doi:10.1007/s12583-015-0578-2.

Shao, L. Y., Zhang, P. F., Hilton, J., et al., 2003. Paleoenvironments and Paleogeography of the Lower and Lower Middle Jurassic Coal Measures in the Turpan-Hami Oil-Prone Coal Basin, Northwestern China. *AAPG Bulletin*, 87(2): 335–355

Wang, J., Shen, G. L., 2000. A New Species of Discinites (Noeggerathiales) from the Upper Permian of Weibei Coalfield, North China. *Review of Palaeobotany and Palynology*, 110(3): 175–190 (in Chinese with English Abstract)

Wang, Z. J., Chen, H. D., Zhang, J. Q., 2002. The Late Palaeozoic Sedimentary Systems and Humic Gas Pools in the Ordos Basin. *Sedimentary Geology and Tethyan Geology*, 22(2): 18–23 (in Chinese with English Abstract)

Wang, F. B., Li, L., Chen, Y. P., 2007. Depositional Models of the Taiyuan Formation in Daniudi Gas Field, the Ordos Basin. *Natural Gas Industry*, 27(12): 49–51 (in Chinese with English Abstract)

Yang, Y. T., Li, W., Ma, L., 2005. Tectonic and Stratigraphic Controls of Hydrocarbon Systems in the Ordos Basin: A Multicycle Cratonic Basin in Central China: *AAPG Bulletin*, 89(2): 255–269

Zhang, G. Q., Chen, S. W., Guo, S. Y., 2011. Sedimentary Facies of the Shanxi Formation in Daniudi Gas Field, Northeastern Ordos Area. *Oil and Gas Geology*, 32(3): 388–396 (in Chinese with English Abstract)